

Article

# A Longitudinal Microcosm Study on the Effects of Ageing on Potential Green Roof Hydrological Performance

Simon De-Ville <sup>1,\*</sup> , Manoj Menon <sup>2</sup> , Xiaodong Jia <sup>3</sup> and Virginia Stovin <sup>4</sup> 

<sup>1</sup> School of Architecture, Building & Civil Engineering, Loughborough University, Loughborough LE11 3TU, UK

<sup>2</sup> Department of Geography, University of Sheffield, Sheffield S10 2TN, UK; M.Menon@sheffield.ac.uk

<sup>3</sup> School of Chemical and Process Engineering, University of Leeds, Leeds LS2 9JT, UK; X.Jia@leeds.ac.uk

<sup>4</sup> Department of Civil & Structural Engineering, University of Sheffield, Sir Frederick Mappin Building, Mappin Street, Sheffield S1 3JD, UK; V.Stovin@sheffield.ac.uk

\* Correspondence: S.De-Ville@lboro.ac.uk; Tel.: +44-1509-22-88-91

Received: 21 May 2018; Accepted: 11 June 2018; Published: 14 June 2018



**Abstract:** Green roofs contribute to stormwater management through the retention of rainfall and the detention of runoff. These processes are reasonably well understood, and runoff responses can be accurately modelled given known system properties. The physical properties of the substrate are particularly relevant to the hydrological response. The substrate is a living biological system, whose properties may change over time. Two sizes of green roof microcosms (50 mm and 150 mm diameter) were observed over a 12-month period. Six system configurations were considered, with two contrasting substrates and three vegetation treatments. Multiple approaches were used to characterize the microcosms' physical and hydrological properties: standard physical tests, bespoke laboratory detention tests, and visualization of the substrate and the root systems using X-ray microtomography. Results suggests that both the substrates' maximum water holding capacity and its capacity to detain runoff tend to increase with age. However, there were inconsistencies in the data and these are discussed within the paper. The noted increases were generally not statistically significant as a result of substrate heterogeneity. Notably, the observed differences after one year were relatively small when compared with differences resulting from original substrate compositions and seasonal changes reported elsewhere.

**Keywords:** green roof; runoff; retention; detention; ageing; substrate; longitudinal

## 1. Introduction

Green roofs can potentially contribute to urban stormwater management through two hydrological processes: the retention of rainfall and the detention of runoff. In temperate climates, it is well known that green roofs tend to retain a higher proportion of rainfall in summer, when there is typically less rainfall and warmer conditions are more favourable for plant growth and evapotranspiration [1]. However, existing studies have been less clear as to whether temporal changes affect a roof's fundamental hydrological properties, i.e., whether the same storm falling on a roof with the same initial moisture content might produce different runoff responses over time due to seasonal and/or aging effects. Berndtsson [2] suggests that the effects of root system development, organic matter turnover, weathering, and substrate consolidation are poorly understood in the context of green roof hydrological performance.

In their extensive review of green roof literature, Li and Babcock [3] identified few studies concerned with ageing. Whilst this partly reflects the scarcity of long-term hydrological records, the

effect that natural climatic variation has on observed hydrological performance is likely to mask any subtle changes in the underlying hydrological characteristics of the system. Measured retention depths rarely reflect the maximum potential retention capacity, as this will only occur if the substrate has reached its permanent wilting point prior to the storm event, and the storm event is sufficiently large to exceed the available capacity such that runoff occurs. Fundamental changes in detention processes are particularly difficult to detect in monitored rainfall/runoff time-series. Reported values such as those for peak attenuation are influenced by rainfall characteristics and antecedent conditions (retention processes) [4]. However, the fundamental hydrological detention processes are essentially independent of these factors and dependent only on the green roof's physical configuration [4]. Therefore, there is a need to focus on the roof's fundamental physical properties rather than on the indirect evidence provided by performance monitoring.

Previous studies that have focused on physical property changes due to ageing have reached inconsistent conclusions. For example, Getter et al. [5] reported increases in the organic matter content of green roof substrates over time, whilst Emilsson and Rolf [6] and Bouzouidja et al. [7] both reported losses. The hydrological implications of these organic matter fluctuations are evidenced in Yio et al. [8], where a threefold increase in organic matter was associated with increases in detention performance (peak attenuation) from 15 to 50%. The pore structure of the substrate matrix is known to dictate hydrological performance [9], yet it remains rarely evaluated as a result of the complex and destructive nature of current test methods. Getter et al. [5] hypothesised improvements to retention performance with an increase in microporosity (pores with a diameter  $<50\ \mu\text{m}$ ); however, this study noted that these improvements may come at the expense of detention performance due to an increased presence of macropore (pores with a diameter  $>50\ \mu\text{m}$ ) channels. The findings of all the above studies were determined through destructive measuring techniques which had been applied to temporally discrete substrate samples. Methodologies based on sequential resampling and destructive testing have inherent limitations for the identification of substrate property changes over time because of the uncertainties associated with sampling highly heterogeneous media.

De-Ville et al. [10] used non-invasive X-ray microtomography (XMT) imaging techniques to compare two contrasting substrate types (one brick-based and the other based on light expanded clay aggregate (LECA)) at two different ages: unused virgin samples and five-year old samples from existing test beds. Image analysis permitted the quantification of a range of physical characteristics that control hydrological performance including solid density, pore size distribution, particle size distribution, and tortuosity. These properties were used to estimate key substrate hydrological characteristics, specifically the maximum water holding capacity (field capacity) and saturated hydraulic conductivity (detention control). Comparisons with physically derived estimates of these properties showed similar values and trends. Conclusions with respect to ageing were that significant long-term changes were not evident in the brick-based substrate, but more marked changes did occur in the LECA-based substrate over time. In particular, its maximum water holding capacity increased by 7% over five years.

Whilst non-invasive XMT imaging potentially removes the problems associated with destructive testing, an acknowledged limitation of the De-Ville et al. [10] study was that different physical samples were used to represent the virgin and aged substrates. As a consequence, there is some uncertainty as to which differences represent changes in the physical characteristics of the substrate over time as opposed to random variations introduced through the natural variability in heterogeneous coarse-grained substrates. These uncertainties can be eliminated by using a longitudinal study of the same substrate samples over time.

To overcome the limitations of discrete temporal sampling De-Ville et al. [11] utilized long term rainfall, runoff, and moisture content records from nine differently configured extensive green roof test beds to determine whether significant changes in potential hydrological performance occurred over time. New methods were proposed to use monitored data to estimate how two of the roof's fundamental physical properties (field capacity and detention control) varied over time. Changes in field capacity were determined from continuous moisture content records, with the apparent field

capacity defined as the moisture content observed in the substrate two hours after the end of a rainfall event that was sufficiently large to generate runoff. Detention control was characterized by fitting reservoir routing model coefficients to observed net rainfall and runoff profiles. Results suggested that seasonal variations in both field capacity and detention characteristics were significantly greater than any long-term ageing effects. The finding that seasonal changes far exceed long-term changes was unexpected but may relate to annual cycles in the green roof's living components (flora and fauna).

However, whilst De-Ville et al. [11] utilized a longitudinal study which included both vegetated and unvegetated systems, changes in physical characteristics could not be directly visualized or measured; instead, they were inferred from monitored rainfall, runoff, and moisture content data. The aim of the work reported in the present paper was to undertake a controlled longitudinal study of green roof microcosms using non-invasive XMT visualization techniques and laboratory measurements of field capacity and detention to directly link these fundamental hydrological characteristics with any changes in physical properties occurring over time.

The longitudinal microcosm study was undertaken in parallel with the long-term monitoring and the cored microcosm studies presented in De-Ville et al. [11] and De-Ville et al. [10], respectively. In this paper, we will present the new findings from the longitudinal microcosm study and draw together findings from the three parallel investigations to reach overall conclusions on the impact of substrate ageing on green roof potential hydrological performance. Further details of the complete research program may be found in De-Ville [12].

## 2. Materials and Methods

The longitudinal microcosm study took place over the course of one full vegetation growing cycle (one year) from August 2015 to August 2016. Two sizes of microcosm were used in the longitudinal study, larger microcosms conforming to the standardized FLL (Forschungsgesellschaft Landschaftsentwicklung Landschaftsbau, Germany) test container guidelines (150 mm diameter, 100 mm depth of substrate) [13], and smaller microcosms suitable for XMT analysis (50 mm diameter, 100 mm depth of substrate). The larger microcosms were used to confirm that the smaller diameter microcosms retained the same bulk physical and hydrological properties as the larger samples.

For each microcosm size, there were two substrate treatments: two vegetation treatments and an unvegetated control, each with three replicates. The two different substrates were a crushed brick-based substrate (BBS) and an expanded clay-based substrate, Figure 1. The BBS is typical of many extensive green roof substrate mixes. The mineral component consists of crushed terracotta brick (55%) and pumice (30%). The organic components are coir (10%) and bark (5%). The second substrate was based on a light expanded clay aggregate (LECA, 80%); the organic component was compost (10%) and loam (10%). The three vegetative treatments were an unvegetated control, a planted sedum vegetation, and a seeded meadow-flower vegetation. Figure 2 shows all of the 50 mm microcosms and a sample of the 150 mm microcosms.

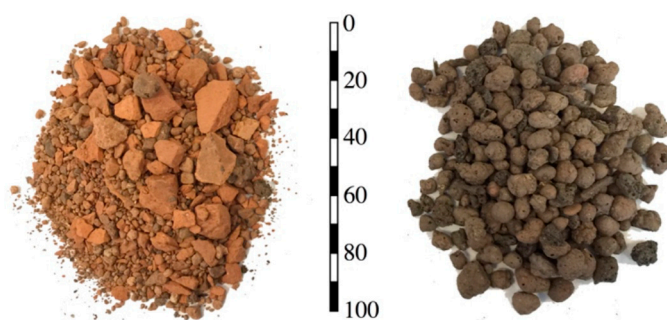


**Figure 1.** (Left) crushed brick-based substrate (BBS); (right) light expanded clay aggregate-based substrate (LECA). The scale is in mm.

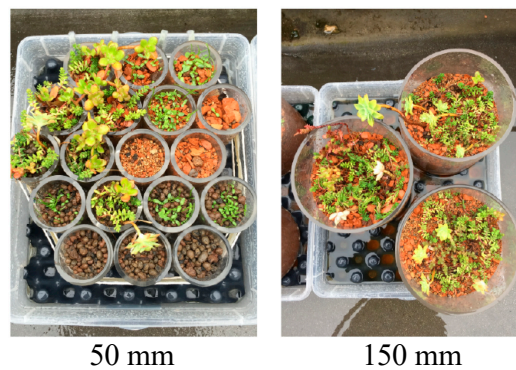


**Figure 2.** Two microcosm sizes. The 150 mm examples are BBS with Sedum vegetation. Image taken 7 October 2015.

All microcosms were tested in accordance with the FLL guidelines [13] for determining apparent density, maximum water holding capacity, saturated hydraulic conductivity, and particle size distribution on the first day of the study (T0) and at the end of the study, one year later (T12). It should be noted that the FLL test for hydraulic conductivity is a basic falling-head test, primarily intended to check compliance with minimum substrate permeability requirements as opposed to providing a definitive scientific measure [14,15].

The 50 mm microcosms were subjected to bespoke laboratory detention testing at T0 and T12. A constant intensity (5 mm/min) 5-min duration ‘rainfall’ was applied to each microcosm using a peristaltic pump and pressure-compensating irrigation dripper. Runoff was monitored using a pressure transducer in a straight-sided collection vessel. Runoff at time  $t$  ( $Q_t$ , mm) is a function of the depth of rainfall temporarily stored in the green roof substrate ( $h$ , mm) via the equation  $Q_t = D_S h_{t-1}^{D_E}$ , in which  $D_S$  ( $\text{mm}^{1-n}$ ) and  $D_E$  (dimensionless) are the reservoir routing scale and exponent, respectively.  $D_E$  was assumed to take a constant value of 2.0 [4,8], whilst  $D_S$  was identified by fitting the modelled runoff profile to the observed runoff. Tests were repeated on each microcosm such that the reported value of  $D_S$  was the mean value based on three replicates. Higher values of  $D_S$  indicated a faster runoff response or a higher apparent hydraulic conductivity. Any change in  $D_S$  from T0 to T12 indicated a change in the microcosm’s fundamental physical properties.

Finally, insights into the physical changes occurring within the substrate were further facilitated by periodic XMT imaging. The 50 mm diameter microcosms were initially imaged in a virgin condition, with no vegetation present, in August 2015, T0. Microcosms were then planted/seeded and allowed to develop under normal external climatic conditions (Sheffield, UK) for eight months before the second images were taken (T8). The third set of images was taken two months later in June 2016 (T10) and the final images set was taken in August 2016 (T12).

XMT imaging was conducted at the University of Nottingham’s Hounsfield Facility for 3D X-ray imaging using a *General Electric Phoenix v|tome|x M* microfocus CT system. All 18 50 mm diameter microcosms were imaged with a spatial resolution of 40  $\mu\text{m}/\text{pixel}$ . All scans were performed at 180 keV and 110  $\mu\text{A}$ , taking 2400 projections (360°) with an exposure time of 250 ms. Total imaging time was 30 min per microcosm, producing ~15 GB of image data per scan.

Image analysis was also undertaken to obtain the following physical properties: porosity (total, effective and ineffective), particle size distribution, pore size distribution, tortuosity, and hydraulic conductivity. Image pre-processing was handled using the ImageJ software [16], and image processing was undertaken using Avizo 9 [17] and ImageJ. Saturated hydraulic conductivity was determined from the 3D XMT image using a Lattice-Boltzmann CFD model (DigiUtility [18]). Full details of the image-processing protocol are provided in De-Ville et al. [10] and De-Ville [12]. The root networks of the ageing cores were analysed where sufficient contrast between the roots and surrounding substrate existed, using the root tracking software RooTrak [19].

Statistically significant differences among the microcosm ages, sizes, and the various treatment groups were analysed using non-parametric Kruskal-Wallis tests with a 0.05 significance level.

### 3. Results

#### 3.1. Effects of Ageing on Physically Derived Substrate Properties

Physical characterizations were performed at the start and the end of the one-year longitudinal microcosm study, for both 50 mm and 150 mm diameter microcosms. Figure 3 presents the physical characterization data for both sizes of microcosm at T0 and T12. Note that, as a result of the buoyant nature of LECA particles which led to substrate disassociation under saturation, it was not always possible to reliably assess the saturated hydraulic conductivity in the LECA-based substrate.

For most properties, Kruskal-Wallis tests indicated no significant differences due to core diameter in the T0 physical analysis. For BBS, there were statistical differences in the particle size distributions and, as a consequence, in the maximum water holding capacity (MWHC), which was higher in the vegetated 150 mm microcosms when compared with the 50 mm microcosms. For the LECA, whilst statistically significant differences in the particle size distributions were also observed, these did not lead to statistically significant differences in the MWHC. Physical recharacterization undertaken at T12 also indicated no significant differences due to core diameter, as at T0.

Figure 3 suggests that comparable changes as a result of ageing were generally observed independently of microcosm size. Increases in MWHC occurred consistently over time in all vegetated microcosms. For the BBS-based microcosms, the mean increase in MWHC was 9.8%. Increased MWHC suggests an increased maximum retention capacity. On the other hand, small increases in saturated hydraulic conductivity were also observed, which would suggest reduced detention (or peak attenuation) capability. Greater variations were observed in the unvegetated (control) microcosms in several properties; this suggests that vegetation may help to stabilize the substrate properties over time.

The physical differences between the two substrates (see Figure 1) suggest that the differences between the two substrates are far greater than the differences associated with microcosm size or age. In comparison with the LECA, the BBS substrate matrix is denser, has a higher MWHC, is better graded and has a lower saturated hydraulic conductivity.

#### 3.2. Detention Performance

Detention performance for the 50 mm microcosms was evaluated using the runoff profiles observed during the 5-min simulated laboratory rainfall events. Detention tests were not undertaken on the LECA-based microcosms because of the previously mentioned tendency of LECA substrates to disassociate due to the buoyant nature of the LECA particles. Figure 4 presents example T0 and T12 rain and runoff profiles for each of the nine BBS microcosms. The detention performance of each microcosm is described through fitted reservoir routing model parameters. The best fit modelled runoff is also illustrated in Figure 4.

Vegetated BBS microcosms exhibited statistically significant reductions in the detention model parameter ( $D_5$ ) from T0 to T12 (Figure 5). The mean value of  $D_5$  for the control microcosms also reduced with time, but this difference was not statistically significant. The reduced values of  $D_5$  indicate an improvement in detention performance; this may also be observed in Figure 4, where the T12 runoff often occurred after the T0 runoff. This observation contradicts the data presented in Figure 3, which suggested that the saturated hydraulic conductivity had increased over time, such that detention performance would have worsened. Further discussion on this is provided later.

$D_5$  values were obtained under a relatively intense rainfall over a short duration. When applying the T0 and T12  $D_5$  values to a more typical design event (e.g., a 1-h duration 30-year return period event), where rainfall intensities are often significantly lower than in the present laboratory case, there was minimal improvement to the storm runoff profile (see De-Ville [12]). Further, when coupled with the dominant effects of retention, these modest detention effects are likely to be imperceptible.

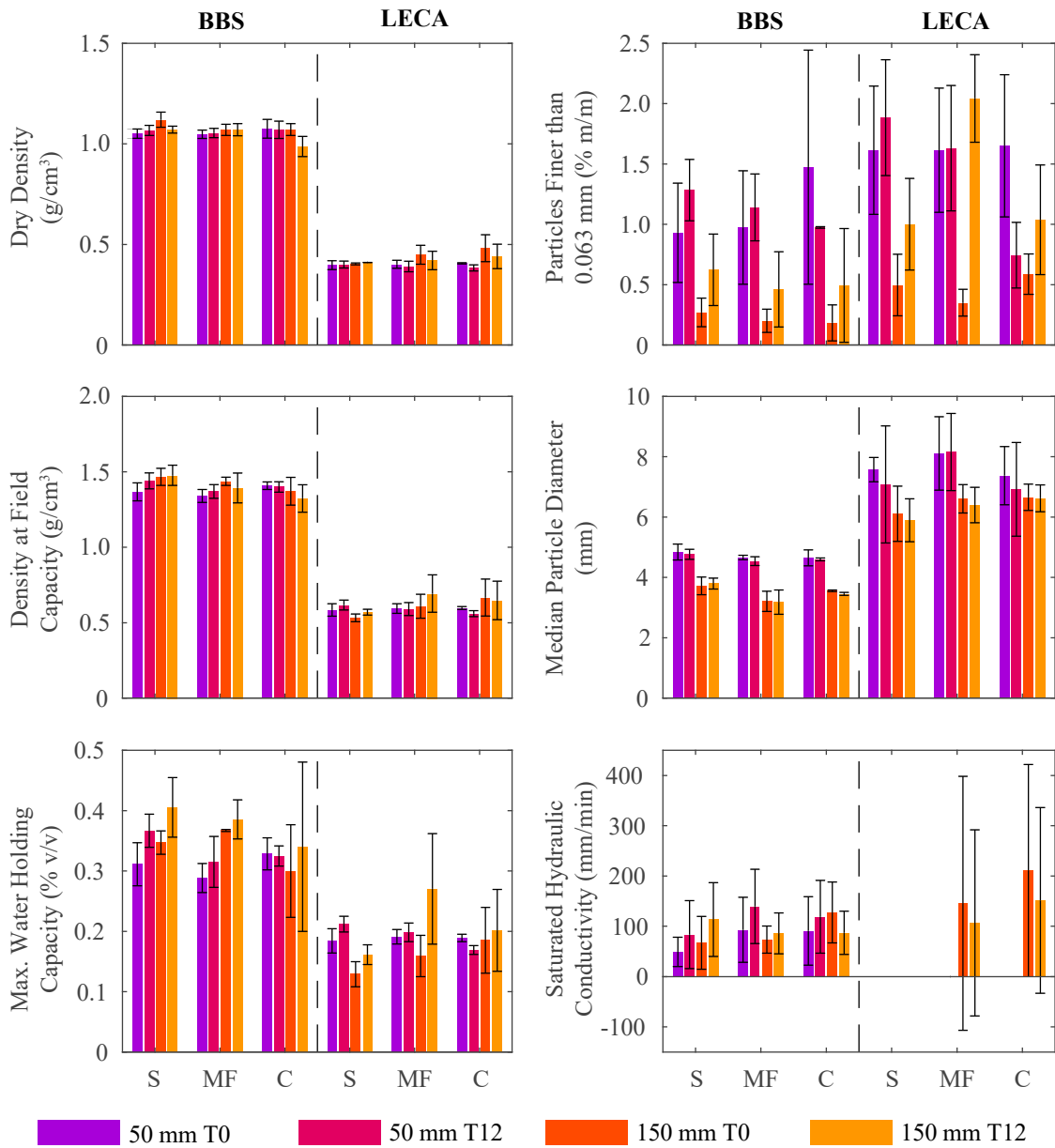


**Figure 3.** Comparison of physically derived properties at the beginning (T0) and end (T12) of the 12-month study period for both 50 mm and 150 mm diameter microsoms. Error bars indicate  $\pm 1$  standard deviations. **S**—Sedum. **MF**—Meadow Flower. **C**—Control.

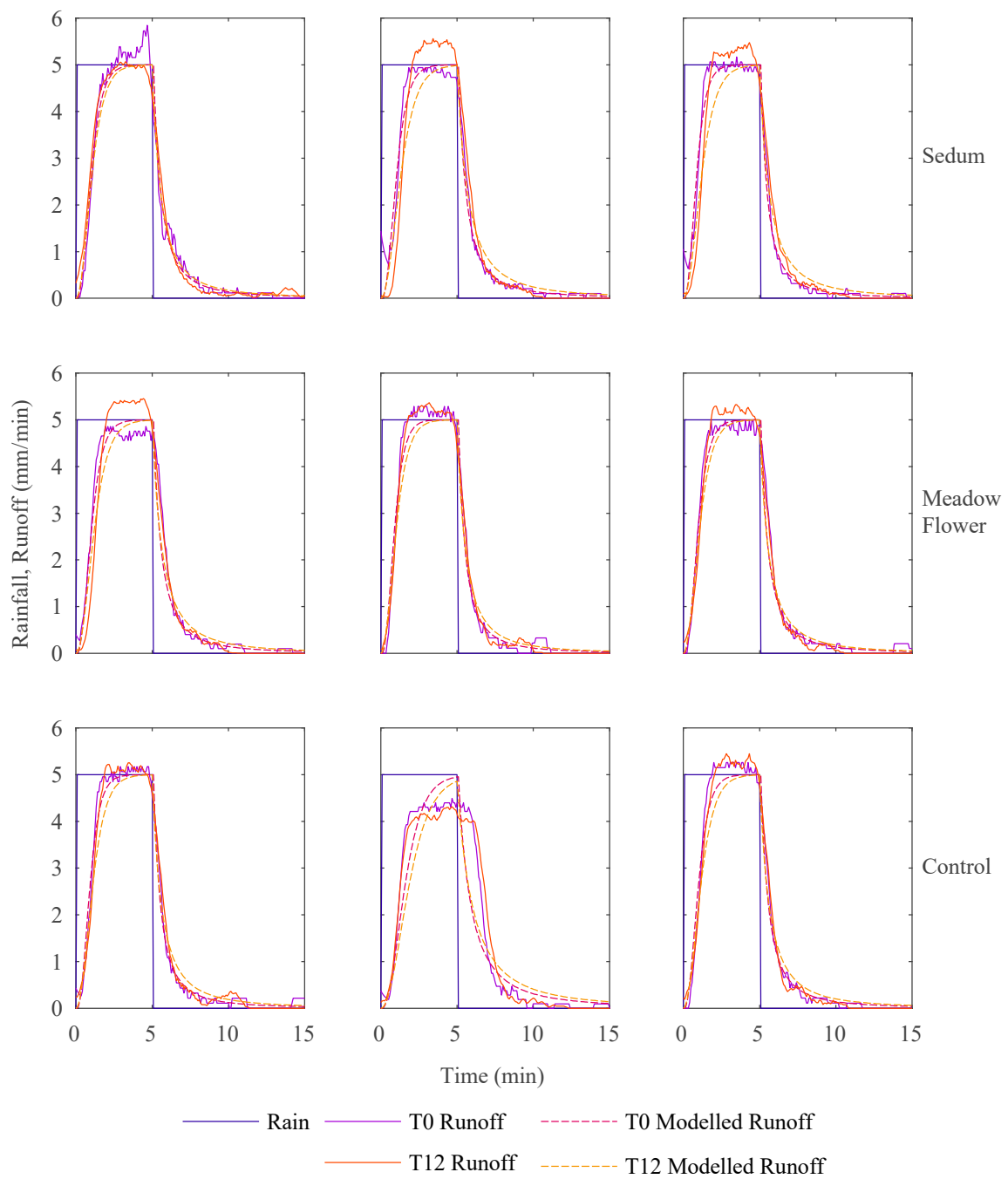


**Figure 4.** Rainfall and runoff from experimental simulated rainfall events on BBS microcosms, including best fit detention model runoff profiles.

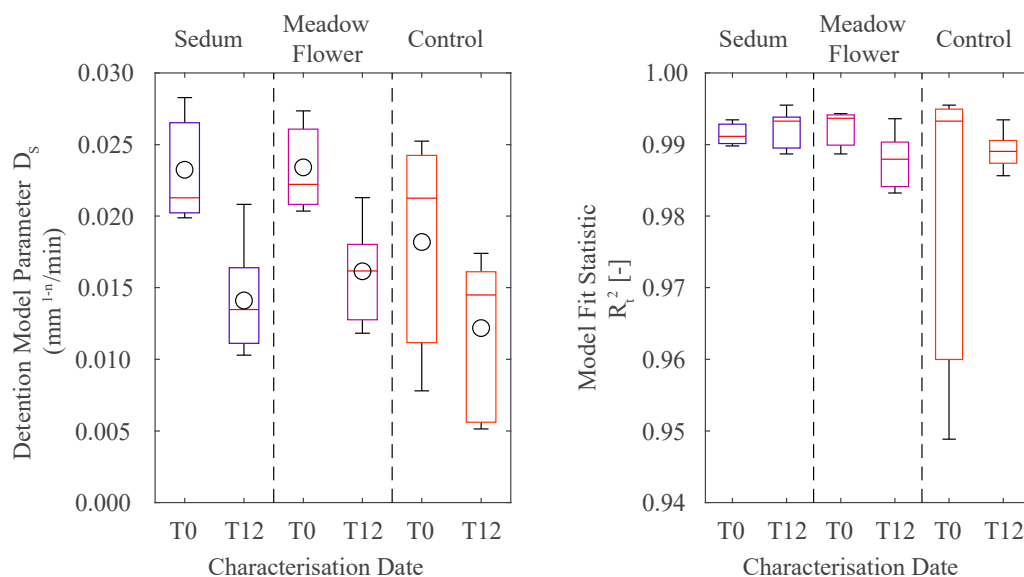


**Figure 5.** (Left) Optimized detention parameter  $D_S$  for BBS 50 mm substrate microcosms at T0 and T12. (Right) Corresponding  $R_i^2$  values for detention parameter  $D_S$ .

### 3.3. XMT Images

The 50 mm microcosms were imaged using XMT four times over the course of the year. T0 and T12 image sets were obtained to tally with the physically derived characterizations. Additional image sets were acquired after eight and 10 months in an attempt to identify changes occurring at a higher temporal resolution. Figures 6 and 7 present sample 2D projections from each of the six treatment groups. The BBS images demonstrate the angular nature of the crushed brick aggregate and the close packing of particles, in a comparison with the more loosely packed, round, LECA particles.

Changes in the matrix over time were difficult to spot, particularly for the BBS substrates. However, there were identifiable differences in the vegetated LECA microcosms from T0 to T8. In the upper left quadrant of the T8 LECA-Sedum image, there is additional material present when compared with T0. This material has fallen through from the upper layers and settled in the available pore space. Similar movement is also observed across the entire LECA-Meadow Flower image set (not shown).

Separated particle images and pore thickness maps were extracted from the unprocessed images (Figures 6 and 7). Particle separation performed well for the BBS substrate, with clearly defined particles that reflect the unprocessed image sets (Figure 6). Separation of the LECA from the wider substrate matrix was less successful (Figure 7). The highly porous nature of the LECA particles resulted in significant subdivision of particles; as such, the separated particle images do not accurately represent the unprocessed images. The exact values of LECA particle sizes are unlikely to represent physically derived measures. The pore thickness maps indicate little difference over time for the BBS cores (Figure 6) but LECA image sets further highlight the movement of material into pore spaces (Figure 7). As seen in the unprocessed images, in the upper-left quadrant of the T8 LECA-Sedum image, pore sizes are much smaller than in the T0 image (Figure 7).



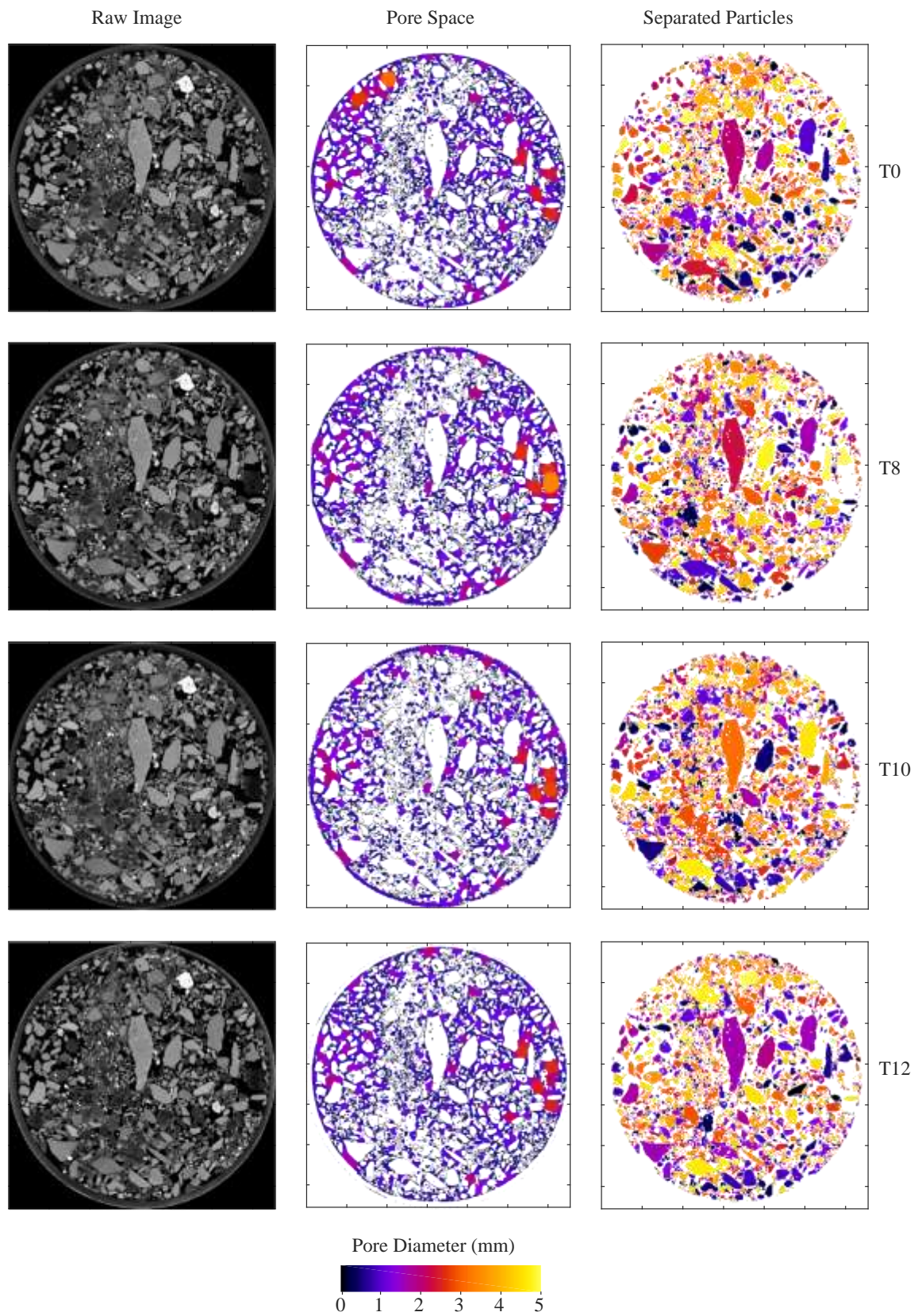


**Figure 6.** Example slices of unprocessed and processed XMT images for the BBS-Sedum substrate microcosms. All images are 52.4 mm across.

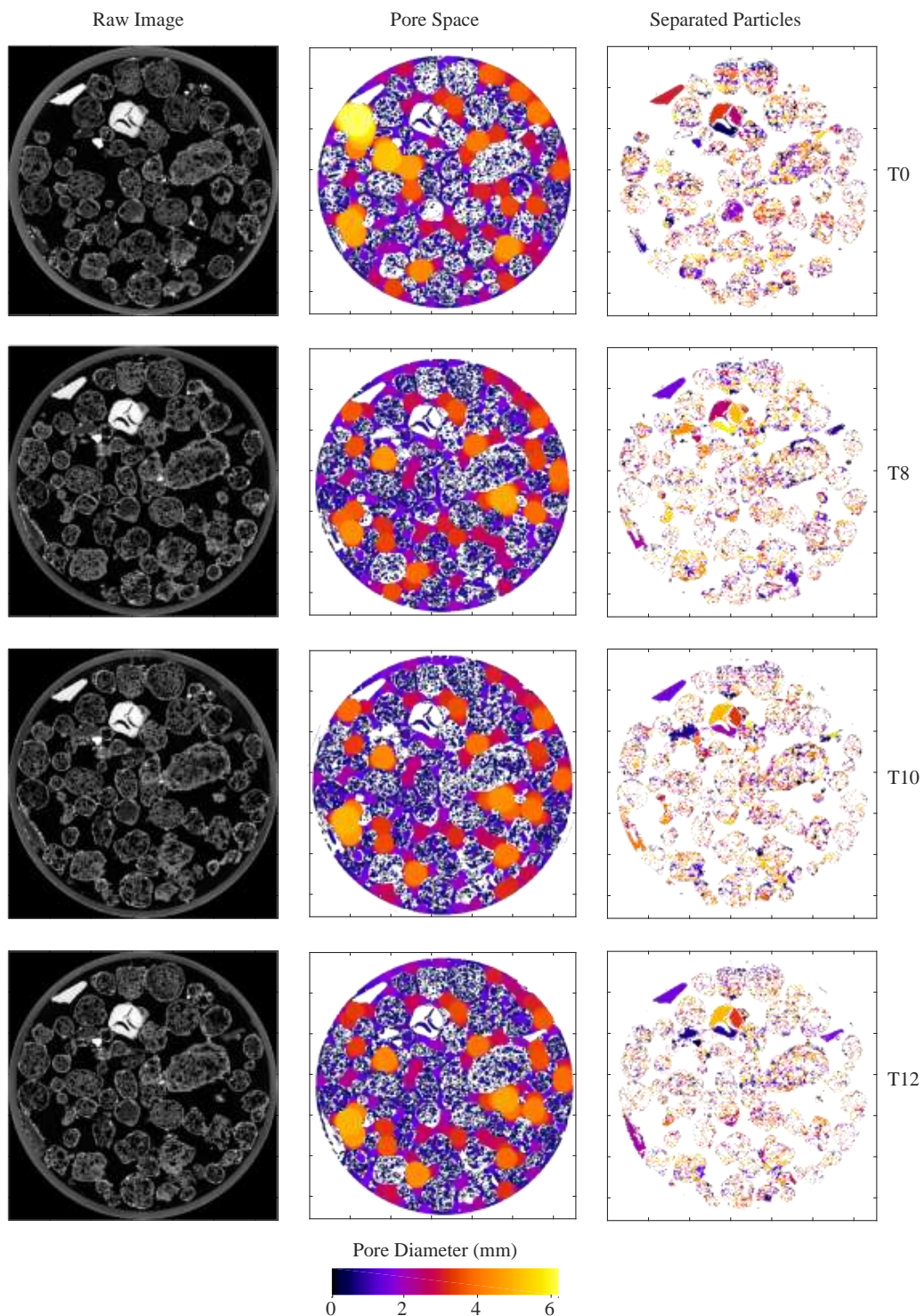


**Figure 7.** Example slices of unprocessed and processed XMT images for LECA-Sedum substrate microcosms. All images are 52.4 mm across.

### 3.3.1. Substrate Root Architecture and Root Growth

The physical and XMT-derived characteristics identified at T0 do not include the effects of vegetation, as all planting/sowing occurred after the initial characterizations took place. Figure 8 illustrates the identified root networks of a Sedum and Meadow Flower BBS microcosm at T8. The rooting systems of the two contrasting vegetation types are clearly very different. Sedum roots are

much denser and extend only to a shallow depth (<30 mm). Meadow Flower roots extend deeper into the substrate, but the network is less dense than that of the Sedum vegetation. In some instances, Meadow Flower roots were observed emerging from the bottom of the microcosm.

The root segmentation in Figure 8 is not perfect; there is some evidence of particles being included in the Meadow Flower root network. These errors arise when there is insufficient contrast between the root material and surrounding aggregate pieces.

Figure 9 illustrates the progressive development of a single BBS root network from T8 to T12. The root network expands significantly in the horizontal plane over time, and root depth extends from 26 mm to 33 mm over four months. Root density may also be observed to have increased.

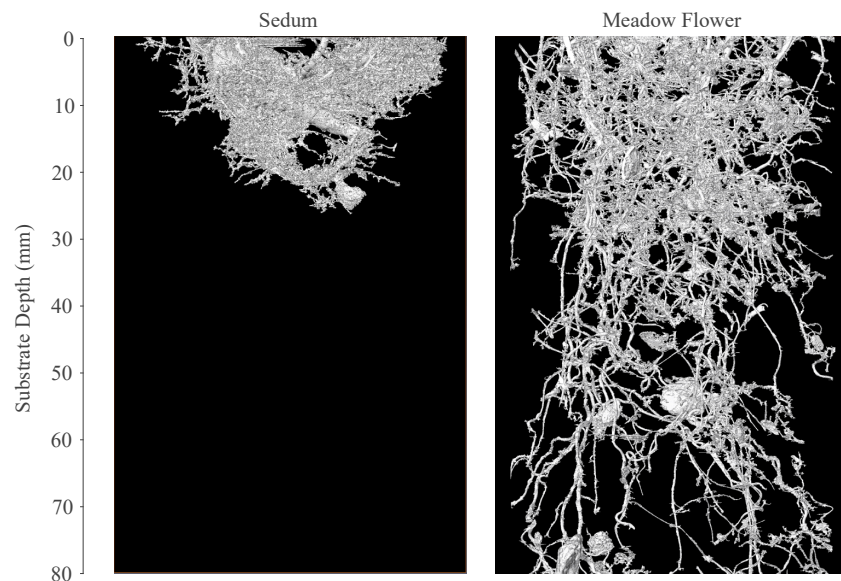


**Figure 8.** 3D volume of surface-connected root networks for Sedum and Meadow Flower vegetation types, identified from XMT data. T8.

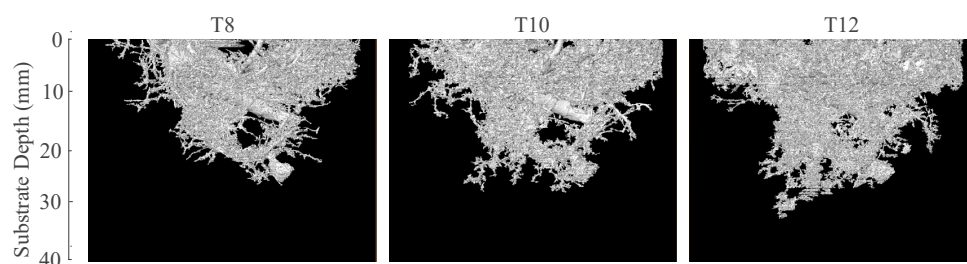


**Figure 9.** 3D volume of surface-connected Sedum root networks over time, identified from XMT images.

The root network characterization has clearly illustrated differences in root network architecture associated with the two different types of vegetation; it has also shown a systematic increase in root extent and density over time. However, earlier analyses suggested that these observable differences have limited effects on the overall physical/hydrological characteristics of the substrate. The effects of the observed differences on the XMT-derived physical properties are explored within the following section.

### 3.3.2. XMT-Derived Properties

The image sets were processed to determine median particle and pore diameters, resolvable porosity, tortuosity, and saturated hydraulic conductivity. Some limitations of the image analysis

(discussed further in De-Ville [12]) suggest that, whilst the data were considered reliable and consistent for the identification of changes over time, absolute values may be expected to differ from those quantified via physical analysis. De-Ville [12] provides a detailed analysis of the derived particle and pore size distributions and tortuosity, which suggests that generally the microcosms demonstrated very little variation over time. Any changes that did occur tended to happen between T0 and T8.

Figure 10 summarizes the XMT-derived properties. Notably, the saturated hydraulic conductivity appears to have decreased over time for all vegetated treatments, with unvegetated BBS increasing marginally and more substantial increases in the unvegetated LECA. This result is different to what was observed in the FLL physical characterization, in which decreases in saturated hydraulic conductivity were identified for the unvegetated control microcosms. However, results are consistent with the values of  $D_5$  derived from the detention experiments. Observed differences between T0 and T12 properties for all microcosms are not statistically different due to the high levels of heterogeneity.

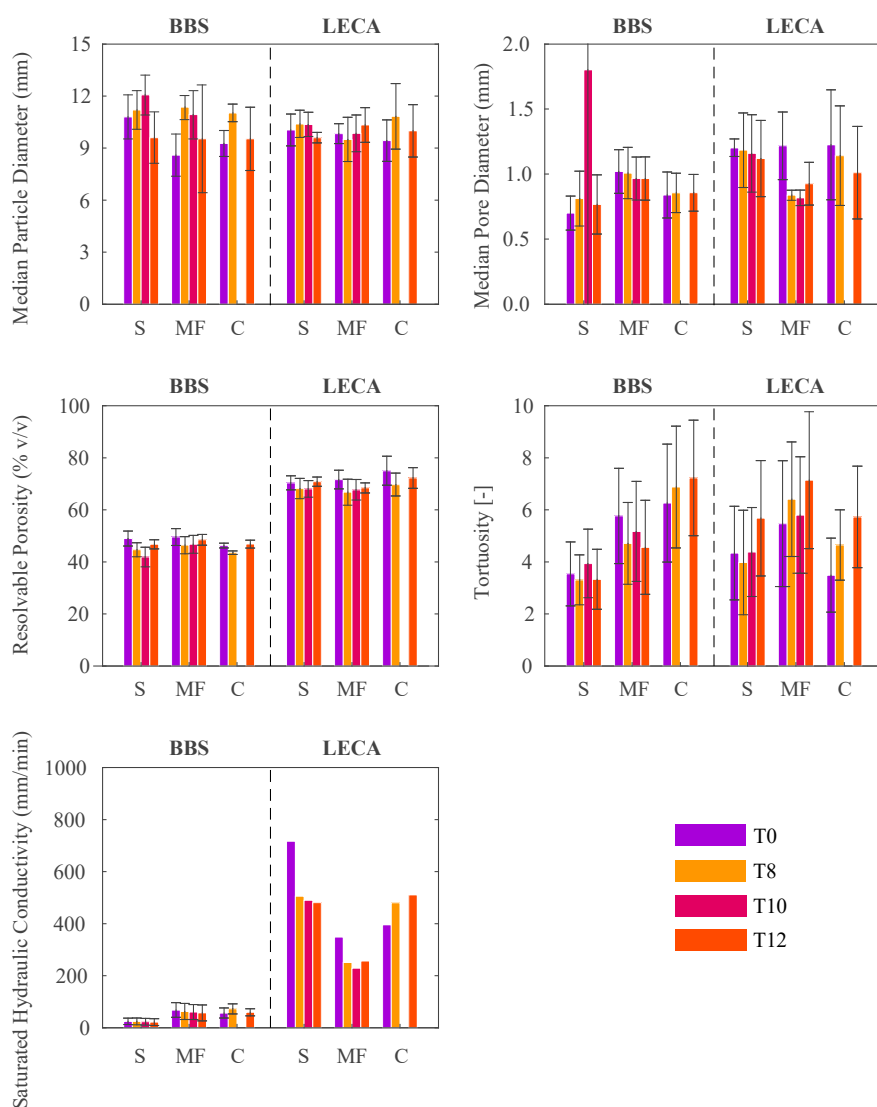


**Figure 10.** Comparison of XMT-derived properties over the course of the 12-month study period. Error bars indicate  $\pm 1$  standard deviations. S—Sedum. MF—Meadow Flower. C—Control.

#### 4. Discussion

The longitudinal microcosm study permitted substrate physical/hydrological properties to be evaluated via physical tests, inference from fitted hydrological model parameters, and non-invasive

X-ray imaging over a 12-month period. All methods have indicated that substrate properties are not constant through time; however, in some cases, the differences are not statistically significant and are not always consistent across different methods of determination. As green roof systems age, many substrate properties are altered via numerous processes, including substrate consolidation, vegetation root growth, organic matter turnover, weathering, atmospheric deposition, and wash-out. Three properties are particularly important for determining substrate hydrological performance (i.e., its retention and detention characteristics): pore size distribution, maximum water holding capacity, and hydraulic conductivity.

#### 4.1. Pore Size Distribution

A substrate's pore size distribution is a controlling factor for many other substrate properties, particularly those important for hydrological performance. The volume of pores with a diameter of less than approximately 50  $\mu\text{m}$  dictates the maximum water holding capacity; pore sizes also control the rate of flow (or permeability) through the media. The XMT-derived median pore diameters exhibited reductions over time in the LECA-based microcosms. This reduction indicates a restructuring of the pore space to include a greater proportion of smaller pores, potentially increasing the total volume of <50  $\mu\text{m}$  pores over time. Complete XMT-derived pore size distributions (not shown here, see De-Ville [12]) suggest that the volume of <50  $\mu\text{m}$  pores does increase over time.

The parallel cored microcosm study [10] also reported increases in the fraction of small pores over time; however, there was greater uncertainty in that study because different samples were considered to represent the virgin and aged material. In the wider literature, Getter et al. [5], Köhler and Poll [20], and Jelinkova et al. [21] all present changes in pore volumes, but do not elaborate with further pore size metrics. Jelinkova et al. [21] used a non-invasive XMT technique to quantify pore networks and observed a reduced total macropore volume near the surface of the substrate. This reduction in macropore volumes is similar to the findings of this study and that of De-Ville et al. [10].

#### 4.2. Maximum Water Holding Capacity (MWHC)

The maximum water holding capacity (equivalent to field capacity) is a controlling factor for green roof retention performance as, in conjunction with the permanent wilting point, it dictates the maximum retention capacity of the green roof. Physical tests undertaken at the start and end of the microcosm study (Figure 3) indicated that increases in MWHC were consistently observed in the vegetated microcosms. This observation is consistent with the changes in pore size distribution reported above. It is also consistent with observations reported in the parallel cored microcosm study [10] and the longer term field monitoring study [11]. The magnitude of changes in MWHC over time are small in comparison to differences associated with various substrate configurations [22]. However, it should be noted that the maximum retention capacity will only be available in practice when the storm event is preceded by a long antecedent dry weather period.

Image resolution limitations of this study prevent the direct indication of MWHC from XMT data. However, even with the highest resolutions available via XMT, there will always be some unresolvable pore spaces. An image resolution better than the pore diameter associated with the matric suction at permanent wilting point (0.2  $\mu\text{m}$  [23]) may permit the evaluation of MWHC from XMT data.

#### 4.3. Saturated Hydraulic Conductivity

Hydraulic conductivity of the substrate governs the rate of runoff from the system, i.e., its detention performance. Notably, green roof substrates are highly permeable. As such, they are not intended/expected to reach saturation, and vertical flow rates through the system will always be lower than indicated by saturated hydraulic conductivity measurements. However, unsaturated hydraulic conductivity varies as a function of substrate moisture content [24] and there are no straightforward established 'in-situ' methods for quantifying this value. Therefore, saturated hydraulic

conductivity provides an indicator of expected relative rates of unsaturated flow and practical detention performance.

Three different approaches were taken. Characterization in LECA-based microcosms was difficult. The physical (FLL) characterizations suggested that hydraulic conductivity in BBS-based microcosms increased with time, whereas both the detention tests and the XMT-based characterization suggested the reverse. Given the comments above regarding the preference for data on unsaturated hydraulic conductivity rather than saturated hydraulic conductivity, and given the acknowledged limitations of the FLL physical test for this parameter [14,15], it may be argued that the physical detention tests provide the most robust estimates of detention performance. The longitudinal microcosm study (Figure 5) suggests that green roof detention performance will tend to improve (to a limited extent) over time.

The long-term monitoring study [11] identified reasonably consistent levels of detention performance in vegetated green roof test beds, whilst unvegetated test beds indicated reduced detention performance with age. Therefore, there are conflicting findings on the overall trend in detention performance with time. However, setting aside the FLL measurements, there is a consensus that, for a typical green roof construction (sedum vegetation on BBS), detention performance does not noticeably deteriorate with system age.

Any subtle changes in the substrate's detention characteristics will tend to be masked by the dominant effects of retention processes. This is clearly illustrated in previously reported hydrological modelling exercises [10,11]. Detention effects due to extensive green roofs are inherently limited because of the shallow nature of the substrate and the requirements for the substrate to offer high rates of permeability to ensure that saturation, waterlogging, or surface overflow do not occur.

#### *4.4. Multiple Lines of Evidence*

The findings of this study and the corresponding De-Ville et al. [10,11] studies complement each other in providing an overall assessment of the changes in substrate properties resulting from system age. The novel identification of a positive trend in the maximum water holding capacity of a substrate over time from monitored substrate moisture content data provides evidence that reducing pore sizes with age increases the total volume of micropores [11]. Micropore volume is critical for moisture retention within the substrate and is the controlling factor for determining the potential retention performance of a green roof system. The application of extensive non-invasive X-ray microtomography to explore the internal structures of green roof substrates for the first time also identified reductions in pore diameters [10].

The identified reduction in pore sizes has led to an increase in substrate maximum water holding capacity over time (De-Ville et al. [10,11]). Such increases forecast an improvement in the potential retention performance of vegetated green roof systems. The reorganisation of the pore space within the substrate is also responsible for small improvements in detention performance over time. Whilst these improvements were only noticeable in this controlled microcosm study, the long-term data record also indicated there was no reduction in detention performance over time for vegetated green roof systems [11].

The coupling of positive trends in retention performance and the absence of negative trends in detention performance suggest that, whilst substrate property changes do occur as a result of ageing, they are unlikely to result in detrimental impacts on overall system hydrological performance. However, observations during the monitoring study identified far greater variations in potential green roof hydrological performance corresponding to a seasonal cycle [11]. There remains a need for a more thorough investigation of the drivers of seasonal changes in the substrate properties that fundamentally control hydrological performance.

## 5. Conclusions

New insights into substrate ageing have been obtained through the establishment of a longitudinal microcosm study alongside previously published indicators of substrate evolution with time. Characterisation of substrate properties, as undertaken physically and via non-invasive X-ray microtomography, indicate that substrate properties responsible for hydrological performance are not constant through time. The magnitude of these changes is determined by the initial substrate composition and the developing vegetation treatment.

The bulk of substrate changes occur within the initial one to two years of a green roof system's lifespan. During this period, substrate consolidation occurs alongside substrate root development, with both processes leading to a reduction of pore sizes within the substrate matrix. This reduction in pore sizes leads to increases in the substrate's maximum water holding capacity and, subsequently, the potential retention performance of the green roof system. A series of complex interacting changes in pore diameters, tortuosity, and saturated hydraulic conductivity lead to improvements in detention performance. Overall, potential hydrological performance is improved due to the combination of these changes to the properties that control retention and detention processes. However, as previously reported [12], the magnitude of these changes is small when compared with seasonal variations.

However, in practice, observed performance is predominantly controlled by weather patterns (rainfall and evapotranspiration rates), and this natural climatic variability will tend to mask any subtle seasonal or longer term changes in substrate properties.

**Author Contributions:** S.D.-V., V.S. and M.M. conceived and designed the experiments; S.D.-V. performed the experiments, analysed, and interpreted the data; X.J. provided technical support for data interpretation. V.S. and S.D.-V. wrote the paper based on data and analysis originally presented in S.D.-V. Ph.D. thesis.

**Funding:** Simon De-Ville was supported by an EPSRC DTA Award (EP/L505055/1). Access to X-ray MicroTomography (XMT) facilities was financially supported by the Pennine Water Group of the University of Sheffield, in turn supported by the Engineering and Physical Sciences Research Council (EPSRC) (grant number EP/I029346/1).

**Acknowledgments:** The authors would like to thank Sacha Mooney and Craig Sturrock from the Hounsfield Facility at the University of Nottingham for the use of their XMT facilities.

**Conflicts of Interest:** The authors declare no conflict of interest.

## References

1. Elliott, R.M.; Gibson, R.A.; Carson, T.B.; Marasco, D.E.; Culligan, P.J.; McGillis, W.R. Green roof seasonal variation: Comparison of the hydrologic behaviour of a thick and a thin extensive system in New York City. *Environ. Res. Lett.* **2016**, *11*, 074020. [[CrossRef](#)]
2. Berndtsson, J.C. Green roof performance towards management of runoff water quantity and quality: A review. *Ecol. Eng.* **2010**, *36*, 351–360. [[CrossRef](#)]
3. Li, Y.; Babcock, R.W. Green roof hydrologic performance and modelling: A review. *Water Sci. Technol.* **2014**, *69*, 727–738. [[CrossRef](#)] [[PubMed](#)]
4. Stovin, V.; Vesuviano, G.; De-Ville, S. Defining green roof detention performance. *Urban Water J.* **2017**, *14*, 574–588. [[CrossRef](#)]
5. Getter, K.L.; Rowe, D.B.; Andresen, J.A. Quantifying the effect of slope on extensive green roof stormwater retention. *Ecol. Eng.* **2007**, *31*, 225–231. [[CrossRef](#)]
6. Emilsson, T.; Rolf, K. Comparison of establishment methods for extensive green roofs in southern Sweden. *Urban For. Urban Green.* **2005**, *3*, 103–111. [[CrossRef](#)]
7. Bouzoudja, R.; Rousseau, G.; Galzin, V.; Claverie, R.; Lacroix, D.; Séré, G. Green roof ageing or Isolatic Technosol's pedogenesis? *J. Soils Sediments* **2018**, *18*, 418–425. [[CrossRef](#)]
8. Yio, M.H.N.; Stovin, V.; Werdin, J.; Vesuviano, G. Experimental analysis of green roof substrate detention characteristics. *Water. Sci. Technol.* **2013**, *68*, 1477–1486. [[CrossRef](#)] [[PubMed](#)]
9. Liu, R.; Fassman-Beck, E. Hydrologic response of engineered media in living roofs and bioretention to large rainfalls: Experiments and modelling. *Hydrol. Process.* **2017**, *31*, 556–572. [[CrossRef](#)]

10. De-Ville, S.; Menon, M.; Jia, X.; Reed, G.; Stovin, V. The impact of green roof ageing on substrate characteristics and hydrological performance. *J. Hydrol.* **2017**, *547*, 332–344. [[CrossRef](#)]
11. De-Ville, S.; Menon, M.; Stovin, V. Temporal variations in the potential hydrological performance of extensive green roof systems. *J. Hydrol.* **2018**, *558*, 564–578. [[CrossRef](#)]
12. De-Ville, S. Hydrological Performance Evolution of Extensive Green Roof Systems. Ph.D. Thesis, The University of Sheffield, Sheffield, UK, 2017.
13. Forschungsgesellschaft Landschaftsentwicklung Landschaftsbau. *Guidelines for the Planning, Construction and Maintenance of Green Roofing—Green Roofing Guideline*; FFL: Bonn, Germany, 2008.
14. Fassman, E.; Simcock, R. Moisture measurements as performance criteria for extensive living roof substrates. *J. Environ. Eng.* **2012**, *138*, 841–851. [[CrossRef](#)]
15. Berretta, C.; Poë, S.; Stovin, V. Moisture content behaviour in extensive green roofs during dry periods: The influence of vegetation and substrate characteristics. *J. Hydrol.* **2014**, *511*, 374–386. [[CrossRef](#)]
16. Schneider, C.A.; Rasband, W.S.; Eliceiri, K.W. NIH Image to ImageJ: 25 years of image analysis. *Nat. Methods* **2012**, *9*, 671–675. [[CrossRef](#)] [[PubMed](#)]
17. FEL. Aviso User's Guide. Available online: <http://www.vsg3d.com/sites/default/files/AvizoUsersGuide.pdf> (accessed on 6 December 2015).
18. SVL, Structure Vision Limited. Available online: <http://www.structurevision.com/digipac.htm> (accessed on 6 December 2015).
19. Mairhofer, S.; Zappala, S.; Tracy, S.R.; Sturrock, C.; Bennett, M.; Mooney, S.J.; Pridmore, T. RooTrak: Automated recovery of three-dimensional plant root architecture in soil from X-ray microcomputed tomography images using visual tracking. *Plant Physiol.* **2012**, *158*, 561–569. [[CrossRef](#)] [[PubMed](#)]
20. Köhler, M.; Poll, P.H. Long-term performance of selected old Berlin greenroofs in comparison to younger extensive greenroofs in Berlin. *Ecol. Eng.* **2010**, *36*, 722–729. [[CrossRef](#)]
21. Jelinkova, V.; Dohnal, M.; Sacha, J. Thermal and water regime studied in a thin soil layer of green roof systems at early stage of pedogenesis. *J. Soils Sediments* **2016**, *16*, 2568–2579. [[CrossRef](#)]
22. Stovin, V.; Poë, S.; De-Ville, S.; Berretta, C. The influence of substrate and vegetation configuration on green roof hydrological performance. *Ecol. Eng.* **2015**, *85*, 159–172. [[CrossRef](#)]
23. Hillel, D. *Introduction to Environmental Soil Physics*; Elsevier Academic Press: Amsterdam, The Netherlands, 2004.
24. Rowell, D. *Soil Science: Methods and Applications*; Longman Scientific & Technical: Harlow, UK, 1994.



© 2018 by the authors. Licensee MDPI, Basel, Switzerland. This article is an open access article distributed under the terms and conditions of the Creative Commons Attribution (CC BY) license (<http://creativecommons.org/licenses/by/4.0/>).